



Review

Progress and Insights in the Application of MXenes as New 2D Nano-Materials Suitable for Biosensors and Biofuel Cell Design

Simonas Ramanavicius ^{1,2} and Arunas Ramanavicius ^{2,*} 

¹ Center for Physical Sciences and Technology (FTMC), Sauletekio av. 3, LT-10257 Vilnius, Lithuania; simonas.ramanavicius@ftmc.lt

² Institute of Chemistry, Department of Physical Chemistry, Faculty of Chemistry and Geosciences, Vilnius University, Naugarduko 24, LT-03225 Vilnius, Lithuania

* Correspondence: Arunas.Ramanavicius@chf.vu.lt; Tel.: +37-06-003-2332

Received: 11 November 2020; Accepted: 29 November 2020; Published: 3 December 2020



Abstract: Recent progress in the application of new 2D-materials—MXenes—in the design of biosensors, biofuel cells and bioelectronics is overviewed and some advances in this area are foreseen. Recent developments in the formation of a relatively new class of 2D metallicly conducting MXenes opens a new avenue for the design of conducting composites with metallic conductivity and advanced sensing properties. Advantageous properties of MXenes suitable for biosensing applications are discussed. Frontiers and new insights in the area of application of MXenes in sensorics, biosensorics and in the design of some wearable electronic devices are outlined. Some disadvantages and challenges in the application of MXene based structures are critically discussed.

Keywords: MXenes; 2D-nanoparticles; 2D-nanomaterials; catalytic electrochemical biosensors; redox enzymes; nonstoichiometric titanium oxides $\text{TiO}_{2-x}/\text{TiO}_2$ and $\text{Ti}_n\text{O}_{2n-1}$; immunosensors; antibodies; enzymatic biofuel cells; microbial biofuel cells; bioelectrochemistry

1. Introduction

MXenes have appeared very recently (in 2011) as a new class of 2D materials with either metallic conductivity [1,2], or some attractive semiconducting properties, or both, which can be well exploited in the design of sensors, biosensors, biofuel cells and in the development of some wearable bioelectronic devices. MXenes have some structural relation and even similarity of some physical properties with other 2D materials such as graphene [3,4]. Most MXenes are based on 2D transition metal carbides [2]. The most of MXenes are based on 2D transition metal nitrides carbonitrides are appointed to this class of MXene materials [5]. MXenes are usually prepared by etching of initial materials, called “MAX phases”, which can be presented by generalized formula $\text{M}_{n+1}\text{AX}_n$ in which “M” representing the transition metals (that are Ti, Sc, Zr, Cr, V, Mn, Hf, Nb, Mo or Ta), “A” is an element from group 12, 13, 14, 15 or 16 (that are Al, Cd, Si, S, P, Ga, As, Ge, In, Tl, Sn or Pb) in the periodic table, “X” is either carbon (C), nitrogen (N) or a mixture of both of them [6–9], and “n” in this formula can be in the range of 1–3 [6,7,9–11] (Figure 1).

1 H Hydrogen 1.008																	2 He Helium 4.003
3 Li Lithium 6.941	4 Be Beryllium 9.012	M										5 B Boron 10.811	6 C Carbon 12.011	7 N Nitrogen 14.007	8 O Oxygen 15.999	9 F Fluorine 18.998	10 Ne Neon 20.180
11 Na Sodium 22.990	12 Mg Magnesium 24.305	A										13 Al Aluminum 26.982	14 Si Silicon 28.086	15 P Phosphorus 30.974	16 S Sulfur 32.066	17 Cl Chlorine 35.453	18 Ar Argon 39.948
19 K Potassium 39.098	20 Ca Calcium 40.078	21 Sc Scandium 44.956	22 Ti Titanium 47.867	23 V Vanadium 50.942	24 Cr Chromium 51.996	25 Mn Manganese 54.938	26 Fe Iron 55.845	27 Co Cobalt 58.933	28 Ni Nickel 58.693	29 Cu Copper 63.546	30 Zn Zinc 65.38	31 Ga Gallium 69.723	32 Ge Germanium 72.63	33 As Arsenic 74.922	34 Se Selenium 78.971	35 Br Bromine 79.904	36 Kr Krypton 84.798
37 Rb Rubidium 84.468	38 Sr Strontium 87.62	39 Y Yttrium 88.906	40 Zr Zirconium 91.224	41 Nb Niobium 92.906	42 Mo Molybdenum 95.95	43 Tc Technetium 98.907	44 Ru Ruthenium 101.07	45 Rh Rhodium 102.906	46 Pd Palladium 106.42	47 Ag Silver 107.868	48 Cd Cadmium 112.414	49 In Indium 114.818	50 Sn Tin 118.710	51 Sb Antimony 121.760	52 Te Tellurium 127.6	53 I Iodine 126.905	54 Xe Xenon 131.294
55 Cs Cesium 132.905	56 Ba Barium 137.328	57-71 Lanthanides	72 Hf Hafnium 178.49	73 Ta Tantalum 180.948	74 W Tungsten 183.84	75 Re Rhenium 186.207	76 Os Osmium 190.23	77 Ir Iridium 192.222	78 Pt Platinum 195.085	79 Au Gold 196.967	80 Hg Mercury 200.592	81 Tl Thallium 204.383	82 Pb Lead 207.2	83 Bi Bismuth 208.980	84 Po Polonium (209)	85 At Astatine (210)	86 Rn Radon (222)
87 Fr Francium (223)	88 Ra Radium (226)	89-103 Actinides	104 Rf Rutherfordium (261)	105 Db Dubnium (262)	106 Sg Seaborgium (266)	107 Bh Bohrium (264)	108 Hs Hassium (265)	109 Mt Meitnerium (268)	110 Ds Darmstadtium (271)	111 Rg Roentgenium (272)	112 Cn Copernicium (285)	113 Nh Nihonium unknown	114 Fl Flerovium (289)	115 Mc Moscovium unknown	116 Lv Livermorium (293)	117 Ts Tennessine unknown	118 Og Oganesson unknown

Figure 1. The composition of MXenes and MAX phases from the periodic table. Reprinted from [12].

It should be noted that MAX phases are characterized by metal-like electrical/thermal conductivity behavior and they are mostly chemically stable materials. MXenes possess great and rather unusual physical and chemical properties that can be well adapted for the design of electrochemical sensors and biosensors. The properties of MXenes can be well tailored through proper variation of M and X elements in MXene structure and by the introduction of various surface terminal groups [13–15]. Due to this option of applying very different surface “finishing”, recent advances in surface chemistry enables the introduction of particular surface “terminal functional groups” [13–15], which can be suitable for the immobilization of enzymes and some other proteins. Hence, MXenes can be efficiently modified by particular biomolecules and many other compounds that are required for the action of biosensors. In addition, the above mentioned “terminal functional groups” can provide tailored electronic, electrochemical and optical properties to MXene-based biosensing structures [13–15]. Optical properties of MXenes are highly applicable for biosensing purposes [16], especially those which are based on fluorescence resonance energy transfer and induce changes in photoluminescence signal [17]; however, the applicability of MXenes in optical biosensors is well reported in specialized review [18], therefore, in this paper we are not aiming to address many details of optical MXene-based biosensors. In some researches [19–27] and reviews [18,28] it is reported, that MXenes are compatible with enzymes and other protein molecules, which are used in the development of catalytic biosensors and affinity sensors. Biocompatibility of MXenes towards some microorganisms [29,30] and even towards mammalian neural cells [31], was also determined. Catalytic activity has been reported for some MXenes, but immobilized enzymes and microorganisms can significantly extend the ability to utilize significantly broader ranges of substrates, which can provide chemical energy for biofuel cells. Bioelectronics devices dependent on the type of applied bio-recognition elements can be divided into several classes, such as: (i) catalytic sensors and biofuel cells based on enzymes [32] and non-enzymatic structures [33], (ii) whole-cell-based biosensors and biofuel cells [34], (iii) affinity sensors based on immobilized antibodies or antigens (immunosensors) [35], (iv) immobilized single stranded DNA (ssDNA)-based sensors (DNA-sensors) [36], molecularly imprinted polymer-based sensors, [37] et cetera. Applicability of various nanomaterials in some of these classes of biosensors has been demonstrated [38]. Some researchers predicted that MXenes will form the basis for various MXene nanocomposites and development of commercially available MXene-based biosensors [39]. Therefore, in this review we are addressing recent advances in the applicability of MXenes in these areas and are predicting future developments in this expanding area.

The aim of this review is to present insights for the applicability of MXenes in the design of biosensors and biofuel cells. A very attractive property of biofuel cells is that they operate at room temperature and are capable of producing electricity from highly diluted solutions of chemical fuels.

2. Catalytic Sensors Based on Enzymes

Catalytic sensors based on enzymes and some other redox proteins have several advantages over other analytical systems because they can provide high selectivity. One of the mostly expanded areas of enzymatic sensors is related to the development of electrochemical sensors and advantages of such sensors are based on low costs, simple operation and ability to being applied for the evaluation of optically badly transparent and turbid samples, for example, blood. Moreover, recently implantable biosensors are appearing in the market and these require biocompatible materials for the design of electrodes and biofuel cells, which will supply power for these implantable devices. Therefore, efficient charge transfer between electrodes and immobilized enzymes is very important issues [40,41]. Moreover, sometimes it is possible to establish direct charge transfer (DCT), which is sometimes called direct electron transfer but this fact is not always correct, because our recent researches show that sometimes DCT is established between p-type semiconducting polymers and redox enzyme, glucose oxidase (GOx) [42,43]. The establishment of direct charge transfer (DCT) between redox enzymes enables exploiting of inherent thermodynamic potential of the enzyme-catalyzed reaction in the design of electrochemical-catalytic biosensors and all types of biofuel cells, which in the most optimal cases are free of soluble redox mediators [40,41,44–46]. Cytochromes can be applied in the design of enzymatic sensors and biofuel cells as catalysts and as redox mediators that are capable of establishing DCT between enzymes and electrodes [32]; and due to this charge-transfer based interaction they can change the optical properties of either Ti_3C_2 MXene based ultra-thin nanosheets, quantum dots, or both, which were applied in the design of biosensors dedicated to the determination of human papilloma virus [47] and trypsin [48]. Charge transfer property was also applied in the design of glucose sensors, where titanium carbide based MXenes were combined with red-emitting carbon dots [49]. Hence, the application of MXenes in DCT-based systems is rather promising; the Nafion stabilized $\text{Ti}_3\text{C}_2\text{T}_x$ -based MXene (where T_x was some transition metal) was applied for sensing of dopamine [50], and electrochemical characterization of glassy carbon electrode (GCE) modified by Nafion (Nafion/ $\text{Ti}_3\text{C}_2\text{T}_x$ /GCE) revealed large surface area, large intrinsic conductivity and low charge transfer resistance. Therefore, it was predicted that MXenes can be well implemented into the construction of enzymatic sensors and biosensors and probably direct charge transfer between MXenes and some redox enzymes can be established. However, establishment of DCT between redox enzymes and solid electrodes is rarely possible, because redox-active sites of most enzymes are rather deeply encapsulated within “electrically insulating” protein structures, which have low electric permittivity (ϵ) [51,52]. Therefore, various soluble redox mediators are applied in the design of such biosensors [53] and biofuel cells [32]. However, soluble redox mediator based strategies are not very efficient, therefore, some conducting nanomaterials including carbon nanotubes [54], gold nanoparticles [44], conducting polymers [55] and very recently, MXenes, can be applied for the purpose of either establishing direct charge transfer between redox enzymes and electrode surfaces, facilitating charge transfer from products formed during enzymatic reaction [56–59], or both. An even more complicated situation is charge transfer from microorganisms because most of them are wrapped within an “electrically insulating” layer of polysaccharides [60,61], but recently we have found how conductivity of cell-walls can be improved by the formation of conducting polymer nanoparticles [60,62] and even some larger structures [61] within the cell wall of microorganisms, and in such a way the conductivity of this initially nonconducting structure can be remarkably improved [34,63]. This formation of conducting polymers can be induced by the metabolic cycle of these microorganisms [64] and conducting polymer-based structures are well distributed within either cell wall, in the periplasm of microorganism [62,65], or both.

Ti_3C_2 -based MXene was used for the immobilization of tyrosinase within the pre-adsorbed chitosan (CS) layer and Tyr/MXene/CS/GCE was applied for the determination of phenol in water with sensitivity of 414.4 mA M, linear range between 0.05–15.5 mM and with LOD of 12 nM [21]. Drop-casting based dispersion was performed and electrostatic effects between MXene and tyrosinase enabled proper orientation of the enzyme during the immobilization and preserved catalytic activity

of immobilized tyrosinase; therefore, very efficient direct charge transfer between tyrosinase and the electrode has been established [19,66].

It should be noted that not only electrons, but holes, can be involved in direct charge transfer within redox enzyme structure and at interphase between enzyme and electrode [42,43], therefore, MXenes in this charge-transfer related context are especially interesting, because they can act as metallic conductors with varied conductivity, which depends on applied “M” and “X” elements in the structure of MXenes ($M_{n+1}X_nT_x$) and covalent surface modifications in their structure [67]. It is remarkable that covalent surface modifications in the structure of MXenes enable achieving superconductivity [67]. The redox-ability, in addition to good conductivity, enables MXenes to facilitate electrochemical redox processes [68]. Hence, some attempts to demonstrate the applicability of MXenes in the design of redox mediator free sensors was demonstrated [19,31] and discussed [5,69], which promises great applicability for MXenes to be applied in various bioelectronics devices including biosensors and biofuel cells. It was demonstrated that if some redox enzymes are trapped within MXene sheets, then rather efficient charge transfer from the active site of enzyme towards electrode can be achieved due to the sufficient mobility of charge within MXene-based structure [70]. In this way β -hydroxybutyrate dehydrogenase decorated MXene nano-sheets were applied for the amperometric determination of β -hydroxybutyrate [71].

MXene and platinum nanoparticle (PtNPs) based nanocomposite was developed and deposited on GCE electrode ($Ti_3C_2T/PtNPs/GCE$) [27], PtNPs significantly enhanced electro-catalytic activity of this MXene-based electrode, and it was sensitive to various compounds that are important during the development of biosensors and biofuel cells, including dopamine, ascorbic acid, uric acid, acetaminophen and H_2O_2 . Such advantageous sensitivity of $Ti_3C_2T/PtNPs/GCE$ electrodes can be potentially adapted for the design of biofuel cell cathodes.

An electrochemical biosensor based on MXene/DNA/Pd/Pt/GCE electrode was developed and applied for amperometric determination of dopamine in the range between 0.2 and 1000 mM with LOD of 30 nM [72]. In this research DNA was important for the dispersion of Ti_3C_2 -based nano-sheets and formation of Pd and Pd/Pt structures, while Ti_3C_2 -based MXene acted as a conducting support. However, this MXene/DNA/Pd/Pt/GCE structure was highly sensitive to glucose, uric acid and ascorbic acid. Therefore, this structure is probably better suited for development of biofuel cells, which will be able to consume much broader ranges of biological fuels.

In many researches it was demonstrated that if electrochemically active surface areas of electrode are not sufficient, then a decoration by metal nanoparticles [52,56,58] or some other nanoparticles can be applied in order to increase catalytic activity and thus the currents registered by electrodes modified by enzymes. A similar strategy was applied during the development of some MXene-based catalytic sensors [31,73]. Ti_3C_2 -based MXene modified by gold nanoparticles (AuNPs) was applied for the Nafion-based immobilization of glucose oxidase (GOx) in order to design a biosensor for the determination of glucose, which was based on Nafion/GOx/AuNPs/ Ti_3C_2/GCE structure [31]. It was predicted that in this structure, AuNPs are involved in charge transfer between the catalytic site of the enzyme and electrode. In another research, GOx was entrapped within three-dimensional porous $Ti_3C_2T_x$ MXene, graphene hybrid films, and also applied for glucose determination [74].

Amperometric biosensor based on acetylcholinesterase (AChE) immobilized on $Ti_3C_2T_x$ and chitosan (CS) modified glassy carbon electrode (AChE/CS/ $Ti_3C_2T_x/GCE$) has been developed and applied for the determination of organophosphorus pesticide—malathion [26]. CS/ $Ti_3C_2T_x$ -based heterostructures provided great environments for the immobilized AChE. A similar AChE/CS/ $Ti_3C_2T_x/GCE$ -heterostructure was applied for the determination of malathion in tap water [73], while acetylcholinesterase (AChE) immobilized on $Ti_3C_2T_x$ modified by silver nanoparticles (AgNPs) was developed and also applied for differential pulse voltammetry (DPV)-based determination of organophosphate pesticide – malathion [75]. In this sensor, negatively charged acetylcholinesterase was electrostatically attracted to the surface of positively charged Ag/ $Ti_3C_2T_x$ -composite, which improved charge transfer from acetylcholinesterase.

Electrochemical biosensors based on acetylcholinesterase, $\text{MnO}_2/\text{Mn}_3\text{O}_4$ micro-cuboids, AuNPs and MXenes ($\text{AChE}/\text{CS}/\text{Ti}_3\text{C}_2/\text{AuNPs}/\text{MnO}_2/\text{Mn}_3\text{O}_4/\text{GCE}$) were developed for the determination of some organophosphate—methamidophos, which has acted as inhibitor of immobilized enzyme—AChE [76]. Some researchers are reporting that anodic potentials, which are exceeding +200 mV, lead to the oxidation of its outer surface of $\text{Ti}_3\text{C}_2\text{T}$ -based MXenes and can be applied for the oxidation of NADH [20]; this remarkable finding is eternally important for the development of enzyme- and microorganism-based biofuel cells because the NAD/NADH system can be served as redox mediator for many enzymes and redox-proteins, and in addition, NAD is a cofactor of NAD-dependent enzymes.

The application of MXenes for the design of catalytic sensors based on enzymes seems rather effective due to metallic conductivity of these compounds.

Ti_3C_2 -based MXene, which was modified by Persian blue (PB), was applied in the design of “wearable” electrochemical biosensors [77] and showed good sensitivity to glucose and lactose applied MXene increased immobilization efficiency of immobilized enzyme, permeability of oxygen into biosensing structure, where it has taken part in the charge transfer from GOx. These sensors were integrated within flexible polymeric structures and used as wearable biosensing devices for the determination of lactose and glucose in actual concentration range of 1–20 mM with the sensitivity of $11.4 \text{ mA} \times \text{mM}^{-1} \times \text{cm}^{-2}$ and $35.3 \text{ mA} \times \text{mM}^{-1} \text{cm}^{-2}$, respectively.

Two types of screen-printed-electrodes: (i) urease, methylene blue (MB), and $\text{Ti}_3\text{C}_2\text{T}_x$ based screen-printed-electrode (urease/MB/MXene/SPE); and (ii) $\text{Ti}_3\text{C}_2\text{T}_x$ based screen-printed-electrode (MXene/SPE) were designed and applied in microfluidic electrochemical systems dedicated to continuous monitoring of urea and creatinine in whole blood were developed [78]. During the development of this biosensor enzyme, urease was immobilized using glutaraldehyde as a cross-linking agent, which binds enzymes well on electrode surfaces [58]. The first electrode based on urease/MB-MXene deposited on a screen printed electrode was used for the determination of urea in the range of 0.1–3 mM and the second one, MXene deposited on screen printed electrode, was used for the determination of creatinine in the range of 0.02–1.2 mM; in this electrode MXene was served as the electro-catalyst. These electrodes are incorporated within a microfluidic system and applied for the determination of urea and creatinine in whole blood. It is very remarkable that some MXenes involved in composite structures are exhibiting peroxidase-like activity and have been applied in the design of biosensors, for example, MXene- $\text{Ti}_3\text{C}_2/\text{CuS}$ nanocomposite based sensor dedicated to colorimetric determination of cholesterol [79] and lactate dehydrogenase (LDH) based heterostructure of a MXene@NiFe-LDH for the detection of glutathione [80].

Nowadays some sensors are implantable; therefore, biocompatibility aspects of such sensors are very important. Here MXenes are especially welcome because some MXenes are biocompatible and almost non-toxic to some living cells such as mouse preosteoblast cell and mouse fibroblast cell lines [81] and mammals such as mice [82]. However, despite some positive results, further investigations on biocompatibility of MXenes in both in vitro and in vivo toxicity assessment based on the determination of either reproductive toxicity, genotoxicity, or both, are needed before the design of implantable MXene-based biosensors and biofuel cells.

3. Direct Charge Transfer between Redox Proteins and MXenes

Direct charge transfer was observed in electrochemical biosensors based on Ti_3C_2 MXene deposited on glassy carbon electrode (GCE) and modified by immobilized hemoglobin (Hb) and Nafion in order to establish a Nafion/Hb/ Ti_3C_2 /MXene/GCE-based structure [22]. This sensor was suitable for the determination of nitrite in water samples. Catalytic activity of NO_2^- reduction in this sensor [19] was based on proton-coupled reaction [83]. The other research group designed a mediator-free enzymatic electrochemical biosensor based on Ti_3C_2 MXene and immobilized hemoglobin and reported the sensitivity of this sensor towards hydrogen peroxide (H_2O_2), with linear range between 0.1 and 260 mM [22]; the authors speculated that this structure exhibits some “organ-like” properties because

it shows high efficiency towards reduction of hydrogen peroxide. This efficiency was achieved due to exfoliation of the MAX-phase, and it was determined that even layers that are thinner than 20 nm still show very high catalytic activity [22]. Exfoliation of separated sheets is observed each time when MXenes are formed [84,85], and there are some evidences that MXenes are providing both compatible environments for immobilized proteins where they retain catalytic activity, very large surface area (Figure 2a) and some functional groups, which can be used for the immobilization of enzymes (Figure 2b) [77].

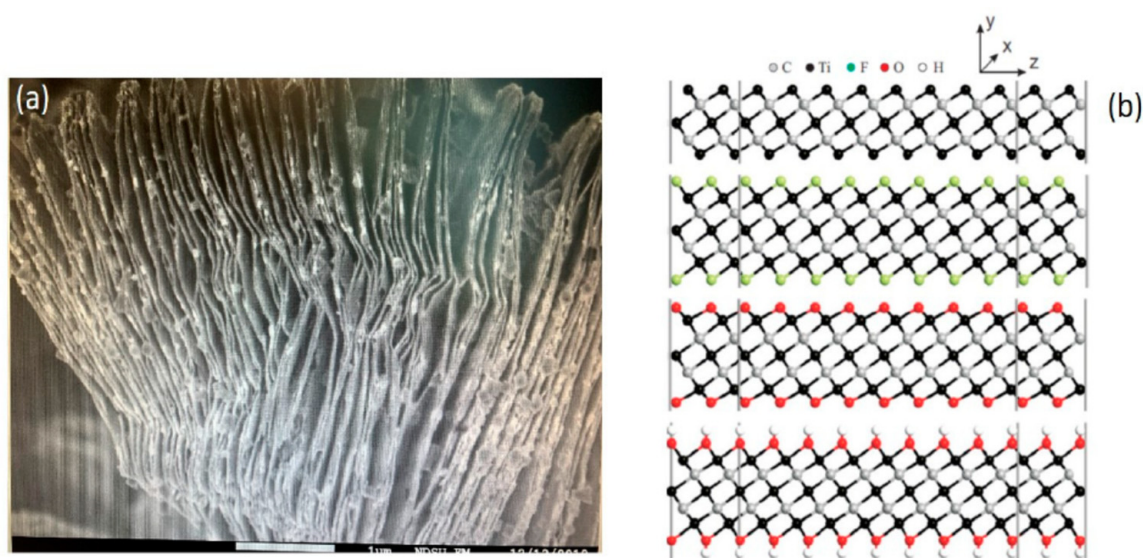


Figure 2. 2D multi-layered Ti_3C_2 MXene sheets (a) scanning electron microscopy image; (b) pristine and surface-terminated Ti_3C_2 MXene with different functional groups. Reprinted from [86].

It should be noted that hemoglobin (Hb) is a very suitable candidate for the development of cathodes for biofuel cells [32]; therefore, this MXene/Hb based electrode seems very pertinent for the design of biofuel cells. It was demonstrated that even better current density can be achieved if, instead of bare Ti_3C_2 , a heterostructure based on TiO_2 - Ti_3C_2 nanocomposite is deposited on the GCE electrode and later it is modified by hemoglobin [22]. In this research, a designed Nafion/Hb/ TiO_2 - Ti_3C_2 -structure based biosensor was characterized by good sensitivity (of $447.3 \text{ mA} \times \text{mM}^{-1} \times \text{cm}^{-2}$) towards H_2O_2 with a linear range of 0.1–380 mM, and LOD of 14 nM [22]. The Nafion/Hb/ TiO_2 - Ti_3C_2 /GCE biosensor [22] showed much better long-term stability in comparison with previously described Nafion/Hb/ Ti_3C_2 /GCE biosensors [22]. It seems that TiO_2 significantly improves the biocompatibility and can advance the conductivity of the formed structure, especially if the nonstoichiometric form of titanium oxide $\text{TiO}_{2-x}/\text{TiO}_2$ is formed, which increases both conductivity and catalytic activity of formed heterostructures [87]. This effect is based on the fact that the $\text{TiO}_{2-x}/\text{TiO}_2^-$ based structure has rather high concentrations of “oxygen vacancies”, which are responsible for n-type charge mobility in this semiconducting heterostructure [88]. Very recently, in one research conducted by our group, we predicted that such oxygen vacancies are providing increased sensitivity towards some reducing and oxidizing gases and VOCs [87]. These TiO_2 -based structures can be reduced and can form nonstoichiometric titanium oxides (TiO_{2-x}), which can be partly based on Magnéli phases with stoichiometry of $\text{Ti}_n\text{O}_{2n-1}$ [89,90]. It was determined that in the TiO_{2-x} structure, which has a rather low “x” value varying between 0 and 0.10, therefore, so called “point defects” dominate in TiO_{2-x} crystal structure [91], and such structures possess high numbers of interstitials based on either Ti^{3+} and Ti^{4+} , great ability of oxygen vacancies, or both. The concentration of above mentioned defects in the crystal structure of TiO_{2-x} is increased by increased “oxygen deficiency” rate. Some researches revealed that in Magnéli phases having rather high “x” values between 0.10 and 0.34 crystallographic shear planes are significantly extended [92]. These TiO_{2-x} heterostructures are

stable, therefore, they are finding many applications in catalytic decontamination of waste-water and in the development of batteries and fuel cells [93,94]. Hence, there are some expectations that these physical properties of $\text{TiO}_{2-x}/\text{TiO}_2$ -based heterostructures will improve performance of some MXene-based sensors and biosensors based on enzymes that are exhibiting direct charge transfer [40,41]. There are some indications that tungsten-based MXenes [95] can be advanced by the incorporation of either stoichiometric, nonstoichiometric tungsten oxide, or both [96,97], and will find some applications in the development of biofuel cells. The application of ink-jet printed MXene with graphene oxide heterocomposite ($\text{Ti}_3\text{C}_2/\text{GO}$) was also modified with Hb [23] and applied in biosensors for the determination of H_2O_2 . Sensitivity of MXenes towards pH [98] can be well exploited in the design of some biosensors based on enzymes with pH that changes during catalytic action.

4. Affinity Sensors Based on MXenes Modified by Immobilized Affinity Agents

Affinity sensors are analytical devices, which specifically recognize analyte and form stable complexes with analytes. According to applied analyte-binding, affinity sensors are classified into immunosensors, DNA-sensors, RNA-sensors and molecularly imprinted polymer based sensors. In some recent researches it was demonstrated that MXenes can be applied in the design of various affinity sensors. A very promising direction here is to design artificial biological recognitions systems based on molecularly imprinted polymers (MIPs) which were developed for proteins [99], DNA-based structures [100], but MIP-based sensors work especially well for the determination of small molecular weight analytes such as caffeine [101], theophylline [102], et cetera. In this research direction, hierarchical porous MXene/amino carbon nanotubes-based molecular imprinting sensor for the determination of low molecular mass analyte, fisetin, has also already been reported [103]. However, larger molecular mass analytes such as proteins were also determined by some MXene-based sensors based on immobilized receptors, for example, Ti_3C_2 -based MXene was modified by biological receptor after the activation with 3-aminopropyl triethoxysilane (APTES) in order to perform covalent binding, and it was applied in the design of affinity sensor [104] for the determination of cancer biomarker, carcinoembryonic antigen [105]. In this research it was reported that the carboxylic group of anti-carcinoembryonic-antibodies binds well to the amino group of $\text{f-Ti}_3\text{C}_2$ MXene and forms a covalent bond. Hexaammineruthenium ($[\text{Ru}(\text{NH}_3)_6]^{3+}$) was applied as a redox-probe for potentiodynamic measurement based determination of analytical signal. Authors declared extremely long linear detection range of this sensor, which was in the range from 10^{-13} to 2×10^{-6} ng/mL with great sensitivity of $37.9 \text{ mA ng/mL} \times \text{cm}^{-2}$ per one decade of concentration with extremely low LOD of 0.000018 ng/mL. This sensor operated well in human serum samples. Application of MXenes for the design of affinity sensors based on antibodies and some other affinity agents offers new avenues for the development of efficient affinity sensors. MXenes were applied for the design of chimeric DNA-functionalized sensors for mapping of some cancer biomarkers in living cells [106] and DNA-sensors suitable for the determination of label-free mismatches of DNA in real human samples [107]. RNA sensors based on the application of MXenes were also reported where a novel label-free electrochemical strategy for the determination of miRNA-182 detection based on $\text{MoS}_2/\text{Ti}_3\text{C}_2$ nanohybrids was applied [108]. microRNA-155 detection based on AuNPs/ Ti_3C_2 MXene three-dimensional nanocomposite for exonuclease III-aided cascade target recycling was designed [109] and oncomiRs detection based on synergetic signal amplification AuNPs/MXene were reported [110]. Very different application of DNA-based structures (such as DNA-aptamers) in the design of bio-recognition elements was applied in sensors dedicated to rapid electrochemical detection of thyroxine [111]. In another research, Ti_3C_2 -based MXene was modified by DNA-aptamer applied in luminol-based chemo-luminescence based affinity sensor for the determination of MCF-7 exosomes [112], which established highly sensitive electro-generated chemo-luminescence. A glassy carbon electrode was modified by poly-nisopropylacrylamide/Au, which has provided a higher concentration of carboxyl available for covalent immobilization of DNA-aptamer, which has selectively recognized MCF-7 exosomes with LOD of 125 particles per mL^{-1} .

Moreover, a label-free electrochemical biosensor for highly sensitive detection of gliotoxin based on DNA nanostructure/MXene nanocomplexes was also reported [113].

MXene-based structures are able to selectively adsorb different molecules through physical adsorption or electrostatic attraction, and lead to a measurable change in the conductivity of the material with high signal-to-noise ratio and excellent sensitivity (Figure 3). Therefore, sensors based on 2-dimensional Ti_3C_2 MXene-based nanosheets were characterized by good sensitivity and selectivity towards PGE2 and 8-HOA, which are both present in A549 lung cancer cells [86].

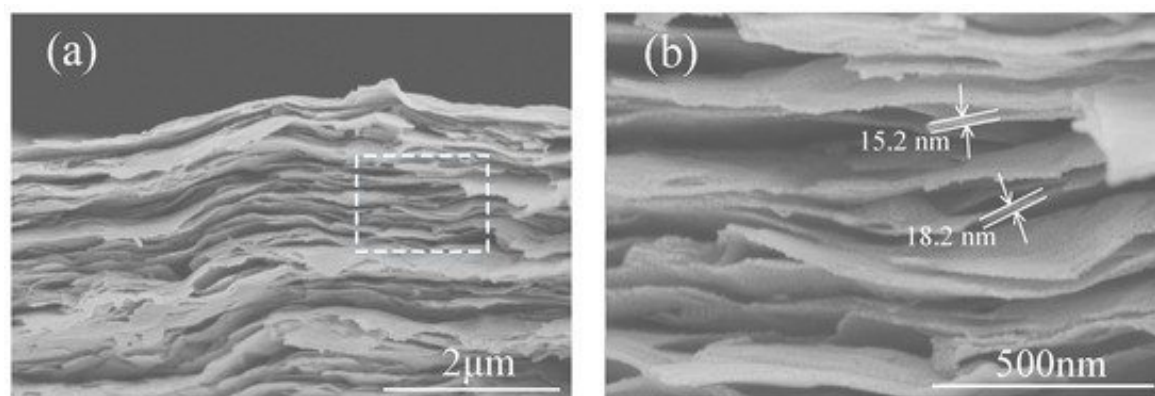


Figure 3. SEM images of (a) a cross-section of $\text{Ti}_3\text{C}_2\text{T}_x$ film and (b) an enlarged part with estimated flake thickness. Reprinted from [114].

5. Non-Enzymatic Biosensors Cell Electrodes

Non-enzymatic biosensors and biofuel cell electrodes are electrochemical systems which are suitable for the determination of biological compounds and catalyze spontaneous oxidation/reduction of various biological compounds by generation of substantial potential (in the range of 50–1200 mV) and electrical current. Nonenzymatic glucose sensors based on application of Ni-nanoparticle/polypyrrole composite was reported recently by our group [33]. The application of MXenes in non-enzymatic glucose sensors also seems very promising as it was demonstrated by the application of three-dimensional porous MXene/NiCo-LDH composite in the design of high performance non-enzymatic glucose sensors [115]. However, despite mentioned achievements, until recently most glucose oxidase (GOx) based sensors used are in this area [40–46], and during catalytic action of GOx as well as by action of many other oxidases hydrogen peroxide (H_2O_2) is produced. Some recent reports in this area illustrate that hydrogen peroxide can be easily determined by non-enzymatic PB/ Ti_3C_2 hybrid nanocomposite [116].

In order to design other non-enzymatic sensors, MXene was introduced into graphite composite paste in order to design (MXene/GCPE)-electrodes, which were sensitive to adrenaline by chronoamperometry with LOD of 9.5 nM [117]. Very efficient determination of adrenaline, serotonin and ascorbic acid was achieved by differential pulse voltammetry (DPV), which enabled separate characteristic DPV-peaks for adrenaline, serotonin and ascorbic acid.

Screen-printed electrodes modified by $\text{Ti}_3\text{C}_2\text{T}_x$ MXene modified (MXene/SPE) were applied for simultaneous detection of acetaminophen and isoniazid drugs [118]. DPV was applied as a detection method, which enabled distinguishing of characteristic DPV-peaks of acetaminophen and isoniazid with linear range between 0.25 and 2000 mM and LOD of 0.048 mM for acetaminophen and linear range between 0.1 and 4.6 mM and LOD of 0.064 mM for isoniazid.

Several MXene-based NH_3 sensors were developed, where the remarkable properties of MXenes to adsorb gaseous materials were well exploited [119,120]. Moreover, catalytic properties of MXenes can be exploited for catalytic determination of various chemical and biochemical compounds [69].

6. Immobilization of Enzymes and Affinity-Agents on MXenes

Oriented immobilization is a very important issue in the design of enzymatic immunosensors and biofuel cells [32]. Well oriented enzymes exhibit sufficient activity, because in such cases the substrate has good access into active sites with lower diffusional limitations in comparison, when the enzyme's active center is oriented upside down and oriented towards the electrode. The only exception is when the direct charge transfer is observed between electrode and enzyme, then the orientation is playing a different role; therefore, the active redox center should be oriented towards the electrode [40,41]. The advantage of MXenes in the application of biofuel cells would be useful for the adsorption of redox enzymes within 2D planes [121–123], because in such a system the orientation of enzymes would play a less critical role and in such a way MXene 2D planes will significantly increase the electrochemically active surface area of electrodes [3]. It is remarkable that MXenes are suitable to be applied for both anodic and cathodic potentials [124]. This property is highly appreciable for the development of biofuel cells because both electrodes can be based on very similar kinds of modifications and can be used for similar enzyme or cell immobilization procedures.

Rather unusual morphology and the ability of MXenes to be split into multiple one dimensional planes [125] (Figures 2 and 3) during the preparation of these materials, enables "to load" MXene-based matrix by high concentrations of enzymes and microorganisms, which together with remarkable metallic conductivity of MXenes increases the applicability of these materials for the design of both enzymatic and microbial biofuel cells. It is remarkable that MXenes offer a good environment for immobilized enzymes or other proteins, which enables retaining sufficient catalytic activity [69,73]. However, up to now, only rather small sheets of MXenes were developed (up to maximum 1 μm in length and width), therefore, they can just be treated as deposits on other substrates.

During the design of immunosensors and affinity sensors, the proper side of the affinity site of antibodies or other receptors should be oriented towards the solution with the analyte, which can be achieved by proper terminal groups of MXenes that are mostly suitable for covalent attachment [13–15]. Some affinity sensors have been designed by the immobilization of affinity-agents by simple adsorption on the surface of working electrode, which was modified by MXene-based sheets [31]. However, this strategy is not very efficient due to the random orientation of these affinity-agents, therefore, improved strategies, which enable orientation of antibodies should be adapted for the development of more efficient affinity sensors [126,127]. A number of such strategies were reported in a targeted review dedicated to the development of immunosensors based on oriented antibodies by Ramanaviciene and Makaraviciute [127] and in their experimental works it was well demonstrated that whole antibodies [128], receptors [129] and some particular parts of antibodies, which were chemically split into two or four pieces [126,127], can be immobilized in oriented-fashion on electrode surfaces. It should be noted that MXenes formed by chemical etching usually possess various surficial functional groups, mostly fluorine ($-\text{F}$) hydroxyl ($-\text{OH}$) or oxygen ($-\text{O}$) [130–132] (Figure 4). It is related to the chemical formula of MXenes, which is " $\text{Mn}+1\text{XnTx}$ ", where T indicates surficial functional groups. Ti_3C_2 MXene formed by chemical etching can be based on the following three structures: $\text{Ti}_3\text{C}_2(\text{OH})_2$, $\text{Ti}_3\text{C}_2\text{O}_2$ and $\text{Ti}_3\text{C}_2\text{F}_2$ (Figure 4) [133]. The quantity and structure of terminal groups is mostly influenced by the synthesis protocol; therefore, the structure of terminal groups can be tailored, which is very important for the covalent immobilization of proteins (e.g., antigens or antibodies), which are used in immunosensor design as biological recognition parts [35].

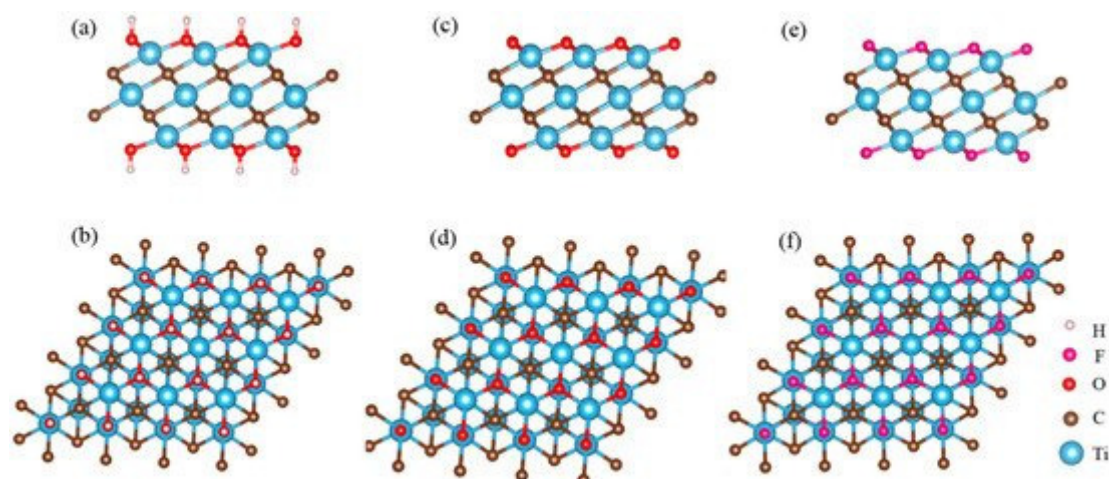


Figure 4. The structure of Ti_3C_2 nanosheets with different functional groups from side and top views: (a,b) $\text{Ti}_3\text{C}_2(\text{OH})_2$; (c,d) $\text{Ti}_3\text{C}_2\text{O}_2$ and (e,f) $\text{Ti}_3\text{C}_2\text{F}_2$. Reprinted from [133].

Ti_3C_2 -based MXene was applied in the design of biomimetic-sensors, which was based on adenosine triphosphate (ATP) deposited on MXene surface and then modified by $\text{Mn}_3(\text{PO}_4)_2$; this system was applied for amperometric determination of superoxide anions (O_2^-) [134], which were generated by HepG2 cells. In this chemical sensor, $\text{Mn}_3(\text{PO}_4)_2$ was sensing superoxide (O_2^-) in the range between 2.5 and 14 mM, sensitivity of $7.86 \text{ mA} \times \text{mM}^{-1} \times \text{cm}^{-2}$ and LOD of 0.5 nM. In addition to amperometric measurements, capacitance measurements can also be applied due to high capacitance storage ability of MXenes; in this direction, Ti_3C_2 MXene nanosheet-based immunoassay with tyramine-enzyme repeating detection of prostate-specific antigens on interdigitated micro-comb electrodes was designed [135].

7. Conclusions and Future Trends

MXenes are 2D-materials, which show real potential for the application in the design of biosensors, biofuel cells and bioelectronics. MXenes are opening a new avenue for the development of conducting composites with metallic conductivity, which can advance sensing properties of amperometric enzymatic biosensors, because direct charge transfer between MXenes and heme-based redox proteins (hemoglobin) has already been reported. This finding opens a new avenue for the design of MXene-based biosensors and biofuel cells with other redox enzymes that are capable of direct charge transfer. Moreover, the advantage of MXenes in the application of biofuel cells would be their ability to adsorb redox enzymes within 2D planes (Figure 2), because in such a system the orientation of enzymes would play a less critical role, and in such way it will significantly increase electrochemically active surface areas of biofuel cell electrodes. The disadvantage of MXenes is that up now, only rather small sheets of MXenes were developed (up to maximum 1 μm in length and width).

Some terminal groups like $-\text{OH}$ can be introduced into MXenes structures, which offers the possibility of immobilizing biological recognition exhibiting proteins in an oriented way; therefore, such ability can be well exploited for oriented immobilization of enzymes and antibodies. However, this property according to our best knowledge was never applied for the immobilization of biological recognition elements required for the design of enzymatic and affinity sensors.

Author Contributions: S.R. performed literature research, analysis, and drafted the paper. A.R. initiated and supervised the work and provided insights. All authors have read and agreed to the published version of the manuscript.

Funding: This research was funded by a grant (No. S-MIP-20-18) from the Lithuanian Research Council.

Conflicts of Interest: The authors declare no conflict of interest.

References

1. Naguib, M.; Kurtoglu, M.; Presser, V.; Lu, J.; Niu, J.; Heon, M.; Hultman, L.; Gogotsi, Y.; Barsoum, M.W. Two-Dimensional Nanocrystals Produced by Exfoliation of Ti_3AlC_2 . *Adv. Mater.* **2011**, *23*, 4248–4253. [[CrossRef](#)]
2. Naguib, M.; Mashtalir, O.; Carle, J.; Presser, V.; Lu, J.; Hultman, L.; Gogotsi, Y.; Barsoum, M.W. Two-dimensional transition metal carbides. *ACS Nano* **2012**, *6*, 1322–1331. [[CrossRef](#)]
3. Naguib, M.; Mochalin, V.N.; Barsoum, M.W.; Gogotsi, Y. 25th Anniversary article, MXenes: A new family of two dimensional materials. *Adv. Mater.* **2014**, *26*, 992–1005. [[CrossRef](#)]
4. Naguib, M.; Gogotsi, Y. Synthesis of two-dimensional materials by selective extraction. *Acc. Chem. Res.* **2015**, *48*, 128–135. [[CrossRef](#)]
5. Deshmukh, K.; Kovárik, T.; Pasha, S.K.K. State of the art recent progress in two dimensional MXenes based gas sensors and biosensors: A comprehensive review. *Coord. Chem. Rev.* **2020**, *424*, 213514. [[CrossRef](#)]
6. Zhao, Y.; Watanabe, K.; Hashimoto, K. Self-supporting oxygen reduction electrocatalysts made from a nitrogen-rich network polymer. *J. Am. Chem. Soc.* **2012**, *134*, 19528–19531. [[CrossRef](#)]
7. Ghidui, M.; Lukatskaya, M.R.; Zhao, M.Q.; Gogotsi, Y.; Barsoum, M.W. Conductive two-dimensional titanium carbide ‘clay’ with high volumetric capacitance. *Nature* **2014**, *516*, 78–81. [[CrossRef](#)]
8. Eklund, P.; Rosen, J.; Persson, P.O.Å. Layered ternary $\text{M}_n\text{+1AX}_n$ phases and their 2D derivative MXene: An overview from a thin-film perspective. *J. Phys. D Appl. Phys.* **2017**, *50*, 113001. [[CrossRef](#)]
9. Magnusan, M.; Mattesini, M. Chemical bonding and electronic-structure in MAX phases as viewed by X-ray spectroscopy and density functional theory. *Thin Solid Films* **2017**, *621*, 108–130. [[CrossRef](#)]
10. Ma, T.Y.; Cao, J.L.; Jaroniec, M.; Qiao, S.Z. Interacting carbon nitride and titanium carbide nanosheets for high performance oxygen evolution. *Angew. Chem. Int. Ed.* **2016**, *55*, 1138–1142. [[CrossRef](#)]
11. She, Z.W.; Fredrickson, K.D.; Anasori, B.; Kibsgaard, J.; Strickler, A.L.; Lukatskaya, M.R.; Gogotsi, Y.; Jaramillo, T.F.; Vojvodic, A. Two-dimensional molybdenum carbide (MXene) as an efficient electrocatalyst for hydrogen evolution. *ACS Energy Lett.* **2016**, *1*, 589–594.
12. Ibrahim, Y.; Mohamed, A.; Abdelgawad, A.M.; Eid, K.; Abdullah, A.M.; Elzatahry, A. The Recent Advances in the Mechanical Properties of Self-Standing Two-Dimensional MXene-Based Nanostructures: Deep Insights into the Supercapacitor. *Nanomaterials* **2020**, *10*, 1916. [[CrossRef](#)]
13. Kim, H.; Wang, Z.; Alshareef, H.N. MXetronics: Electronic and photonic applications of MXenes. *Nano Energy* **2019**, *60*, 179–197. [[CrossRef](#)]
14. Khazaei, M.; Arai, M.; Sasaki, T.; Ranjbar, A.; Liang, Y.; Yunoki, S. OH-terminated two-dimensional transition metal carbides and nitrides as ultralow work function materials. *Phys. Rev.* **2015**, *B 92*, 075411. [[CrossRef](#)]
15. Tahini, H.A.; Tan, X.; Smith, S.C. The origin of low work functions in OH terminated MXenes. *Nanoscale* **2017**, *9*, 7016–7020. [[CrossRef](#)]
16. Liu, M.; He, Y.; Zhou, J.; Ge, Y.; Zhou, J.; Song, G. A “naked-eye” colorimetric and ratiometric fluorescence probe for uric acid based on Ti_3C_2 MXene quantum dots. *Anal. Chim. Acta* **2020**, *1103*, 134–142. [[CrossRef](#)]
17. Zhang, Q.; Wang, F.; Zhang, H.; Zhang, Y.; Liu, M.; Liu, Y. Universal Ti_3C_2 MXenes Based Self-Standard Ratiometric Fluorescence Resonance Energy Transfer Platform for Highly Sensitive Detection of Exosomes. *Anal. Chem.* **2018**, *90*, 12737–12744. [[CrossRef](#)]
18. Zhu, X.; Zhang, Y.; Liu, M.; Liu, Y. 2D titanium carbide MXenes as emerging optical biosensing platforms. *Biosens. Bioelectron.* **2021**, *171*, 112730. [[CrossRef](#)]
19. Liu, H.; Duan, C.; Yang, C.; Shen, W.; Wang, F.; Zhu, Z. A novel nitrite biosensor based on the direct electrochemistry of hemoglobin immobilized on MXene- Ti_3C_2 . *Sens. Actuat. B* **2015**, *218*, 60–66. [[CrossRef](#)]
20. Lorencova, L.; Bertok, T.; Dosekova, E.; Holazova, A.; Paprckova, D.; Vikartoska, A.; Sasinkova, V.; Filip, J.; Kasak, P.; Jerigova, M.; et al. Electrochemical performance of $\text{Ti}_3\text{C}_2\text{T}_x$ MXene in aqueous media: Towards ultrasensitive H_2O_2 sensing. *Sens. Actuat. B* **2017**, *235*, 471–479. [[CrossRef](#)]
21. Wu, L.; Lu, X.; Dhanjai, Z.S.; Wu, Y.; Dong, X.; Wang, S.; Zheng, J.C. 2D transition metal carbide MXene as a robust biosensing platform for enzyme immobilization and ultrasensitive detection of phenol. *Biosens. Bioelectron.* **2018**, *107*, 69–75. [[CrossRef](#)]
22. Wang, F.; Yang, C.; Duan, C.; Xiao, D.; Tang, Y.; Zhu, J. An organ-like titanium carbide material (MXene) with multilayer structure encapsulating hemoglobin for a mediator-free biosensor. *J. Electrochem. Soc.* **2015**, *162*, B16–B21. [[CrossRef](#)]

23. Zheng, J.; Diao, J.; Jin, Y.; Ding, A.; Wang, B.; Wu, L.; Wong, B.; Chen, J. An inkjet printed $\text{Ti}_3\text{C}_2\text{-GO}$ electrode for the electrochemical sensing of hydrogen peroxide. *J. Electrochem. Soc.* **2018**, *165*, B227–B231. [[CrossRef](#)]
24. Zhu, X.; Liu, B.; Hou, H.; Huang, Z.; Zeinu, K.M.; Huang, L.; Yuan, X.; Guo, D.; Hu, J.; Yang, J. Alkaline intercalation of Ti_3C_2 MXene for simultaneous electrochemical detection of Cd(II), Pb(II), Cu(II) and Hg(II). *Electrochim. Acta* **2017**, *248*, 46–57. [[CrossRef](#)]
25. Rasheed, P.A.; Pandey, R.P.; Rasool, K.; Mahmoud, K.A. Ultra-sensitive electrocatalytic detection of bromate in drinking water based on Nafion/ $\text{Ti}_3\text{C}_2\text{T}_x$ (MXene) modified glassy carbon electrode. *Sens. Actuat. B* **2018**, *265*, 652–659. [[CrossRef](#)]
26. Zhou, L.; Zhang, X.; Ma, L.; Gao, J.; Jiang, Y. Acetylcholinesterase/chitosan transition metal carbides nanocomposites-based biosensor for the organophosphate pesticides detection. *Biochem. Eng. J.* **2017**, *128*, 243–249. [[CrossRef](#)]
27. Lorencova, L.; Bertok, T.; Filip, J.; Jerigova, M.; Elic, D.; Kasak, P.; Ahmoud, K.A.; Tkac, J. Highly stable $\text{Ti}_3\text{C}_2\text{T}_x$ (MXene)/Pt nanoparticles-modified glassy carbon electrode for H_2O_2 and small molecules sensing applications. *Sens. Actuat. B* **2018**, *263*, 360–368. [[CrossRef](#)]
28. Kalambate, P.K.; Gadhari, N.S.; Li, X.; Rao, Z.; Navale, S.T.; Shen, Y.; Patil, V.R.; Huang, Y. Recent advances in MXene-based electrochemical sensors and biosensors. *TrAC Trends Anal. Chem.* **2019**, *120*, 115643. [[CrossRef](#)]
29. Rasool, K.; Mahmoud, K.A.; Johnson, D.J.; Helal, M.; Berdiyrov, G.R.; Gogotsi, Y. Efficient Antibacterial Membrane based on Two-Dimensional $\text{Ti}_3\text{C}_2\text{T}_x$ (MXene) Nanosheets. *Sci. Rep.* **2017**, *7*, 1598. [[CrossRef](#)]
30. Lin, H.; Chen, Y.; Shi, J. Insights into 2D MXenes for Versatile Biomedical Applications: Current Advances and Challenges Ahead. *Adv. Sci.* **2018**, *5*, 1800518. [[CrossRef](#)]
31. Rakhi, R.B.; Nayak, P.; Xia, C.; Alshareef, H.N. Novel amperometric glucose biosensor based on MXene nanocomposite. *Sci. Rep.* **2016**, *6*, 36422. [[CrossRef](#)]
32. Ramanavicius, A.; Ramanaviciene, A. Hemoproteins in design of biofuel cells. *Fuel Cells* **2009**, *9*, 25–36. [[CrossRef](#)]
33. Emir, G.; Dilgin, Y.; Ramanaviciene, A.; Ramanavicius, A. Amperometric Nonenzymatic Glucose Biosensor based on Graphite Rod Electrode Modified by Ni-Nanoparticle/Polypyrrole Composite. *Microchem. J.* **2020**, in press. [[CrossRef](#)]
34. Kisieliute, A.; Popov, A.; Apetrei, R.M.; Cârâc, G.; Morkvenaite-Vilkonciene, I.; Ramanaviciene, A.; Ramanavicius, A. Towards Microbial Biofuel Cells: Improvement of Charge Transfer by Self-Modification of Microorganisms with Conducting Polymer—Polypyrrole. *Chem. Eng. J.* **2019**, *356*, 1014–1021. [[CrossRef](#)]
35. Ramanavicius, A.; Oztekin, Y.; Ramanaviciene, A. Electrochemical Formation of Polypyrrole-based Layer for Immunosensor Design. *Sens. Actuators B Chem.* **2014**, *197*, 237–243. [[CrossRef](#)]
36. Ramanaviciene, A.; Ramanavicius, A. Pulsed amperometric detection of DNA with an ssDNA/polypyrrole modified electrode. *Anal. Bioanal. Chem.* **2004**, *379*, 287–293. [[CrossRef](#)]
37. Ratautaite, V.; Plausinaitis, D.; Baleviciute, I.; Mikoliunaite, L.; Ramanaviciene, A.; Ramanavicius, A. Characterization of Caffeine-Imprinted Polypyrrole by a Quartz Crystal Microbalance and Electrochemical Impedance Spectroscopy. *Sens. Actuators B Chem.* **2015**, *212*, 63–71. [[CrossRef](#)]
38. Glenn, E.; Fryxell, G.C. *Environmental Applications of Nanomaterials: Synthesis, Sorbents and Sensors*, 2nd ed.; Imperial Collage Press: London, UK, 2012.
39. Yoon, J.; Shin, M.; Lim, J.; Lee, J.-Y.; Choi, J.W. Recent Advances in MXene Nanocomposite-Based Biosensors. *Biosensors* **2020**, *10*, 185. [[CrossRef](#)]
40. Oztekin, Y.; Ramanaviciene, A.; Yazicigil, Z.; Solak, A.O.; Ramanavicius, A. Direct electron transfer from glucose oxidase immobilized on polyphenanthroline modified-glassy carbon electrode. *Biosens. Bioelectron.* **2011**, *26*, 2541–2546. [[CrossRef](#)]
41. Kausaite-Minkstimiene, A.; Mazeiko, V.; Ramanaviciene, A.; Oztekin, Y.; Solak, A.O.; Ramanavicius, A. Evaluation of some redox mediators in the design of reagentless amperometric glucose biosensor. *Electroanalysis* **2014**, *26*, 1528–1535. [[CrossRef](#)]
42. Bagdžiūnas, G.; Ramanavičius, A. Towards Direct Enzyme Wiring: A Theoretical Investigation of Charge Carriers Transfer Mechanisms between Glucose Oxidase and Organic Semiconductors. *Phys. Chem. Chem. Phys.* **2019**, *21*, 2968–2976. [[CrossRef](#)] [[PubMed](#)]
43. Bagdžiūnas, G.; Žukauskas, Š.; Ramanavičius, A. Insights into Hole Transfer Mechanism between Glucose Oxidase and p-Type Organic Semiconductor. *Biosens. Bioelectron.* **2018**, *102*, 449–455. [[CrossRef](#)]

44. Ramanaviciene, A.; Nastajute, G.; Snitka, V.; Kausaite, A.; German, N.; Barauskas-Memenas, D.; Ramanavicius, A. Spectrophotometric evaluation of gold nanoparticles as red-ox mediator for glucose oxidase. *Sens. Actuators B Chem.* **2009**, *137*, 483–489. [[CrossRef](#)]
45. Ramanavicius, A.; Kausaite, A.; Ramanaviciene, A. Enzymatic biofuel cell based on anode and cathode powered by ethanol. *Biosens. Bioelectron.* **2008**, *24*, 761–766. [[CrossRef](#)] [[PubMed](#)]
46. Ramanavicius, A.; Kausaite, A.; Ramanaviciene, A. Biofuel cell based on direct bioelectrocatalysis. *Biosens. Bioelectron.* **2005**, *20*, 1962–1967. [[CrossRef](#)]
47. Peng, X.; Zhang, Y.; Lu, D.; Guo, Y.; Guo, S. Ultrathin Ti₃C₂ nanosheets based “off-on” fluorescent nanoprobe for rapid and sensitive detection of HPV infection. *Sens. Actuator B Chem.* **2019**, *286*, 222–229. [[CrossRef](#)]
48. Liu, M.; Zhou, J.; He, Y.; Cai, Z.; Ge, Y.; Zhou, J.; Song, G. “-Poly-L-lysine-protected Ti₃C₂ MXene quantum dots with high quantum yield for fluorometric determination of cytochrome c and trypsin. *Microchim. Acta* **2019**, *186*, 770. [[CrossRef](#)]
49. Zhu, X.H.; Pang, X.; Zhang, Y.Y.; Yao, S.Z. Titanium carbide MXenes combined with red-emitting carbon dots as a unique turn-on fluorescent nanosensor for label-free determination of glucose. *J. Mater. Chem. B* **2019**, *7*, 7729–7735. [[CrossRef](#)]
50. Shahzad, F.; Iqbal, A.; Zaidi, S.A.; Hwang, S.W.; Koo, C.M. Nafion-stabilized twodimensional transition metal carbide (Ti₃C₂T_x MXene) as a high-performance electrochemical sensor for neurotransmitter. *J. Indus. Eng. Chem.* **2019**, *79*, 338–344. [[CrossRef](#)]
51. Lapenaite, I.; Ramanaviciene, A.; Ramanavicius, A. Current trends in enzymatic determination of glycerol. *Crit. Rev. Anal. Chem.* **2006**, *36*, 13–25. [[CrossRef](#)]
52. German, N.; Ramanaviciene, A.; Ramanavicius, A. Formation of Polyaniline and Polypyrrole Nanocomposites with Embedded Glucose Oxidase and Gold Nanoparticles. *Polymers* **2019**, *11*, 377. [[CrossRef](#)]
53. Kausaite-Minkstimiene, A.; Glumbokaite, L.; Ramanaviciene, A.; Dauksaite, E.; Ramanavicius, A. An amperometric glucose biosensor based on poly(pyrrole-2-carboxylic acid)/glucose oxidase biocomposite. *Electroanalysis* **2018**, *30*, 1642–1652. [[CrossRef](#)]
54. Bruzaite, I.; Rozene, J.; Morkvenaite-Vilkonciene, I.; Ramanavicius, A. Towards Microorganism-based Biofuel Cells: The Viability of *Saccharomyces cerevisiae* Modified by Multiwalled Carbon Nanotubes. *Nanomaterials* **2020**, *10*, 954. [[CrossRef](#)]
55. Kausaite-Minkstimiene, A.; Glumbokaite, L.; Ramanaviciene, A.; Ramanavicius, A. Reagent-less amperometric glucose biosensor based on nanobiocomposite consisting of poly(1,10-phenanthroline-5,6-dione), poly(pyrrole-2-carboxylic acid), gold nanoparticles and glucose oxidase. *Microchem. J.* **2020**, *154*, 104665. [[CrossRef](#)]
56. German, N.; Ramanavicius, A.; Voronovic, J.; Oztekin, Y.; Ramanaviciene, A. The effect of gold nanoparticle colloidal solution on performance of glucose oxidase modified carbon electrode. *Microchim. Acta* **2011**, *172*, 185–191. [[CrossRef](#)]
57. German, N.; Ramanavicius, A.; Voronovic, J.; Ramanaviciene, A. Glucose biosensor based on glucose oxidase and gold nanoparticles of different sizes covered by polypyrrole layer. *Colloids Surf. A Physicochem. Eng. Asp.* **2012**, *413*, 224–230. [[CrossRef](#)]
58. German, N.; Ramanaviciene, A.; Ramanavicius, A. Electrochemical deposition of gold nanoparticles on graphite rod for glucose biosensing. *Sens. Actuators B Chem.* **2014**, *203*, 25–34. [[CrossRef](#)]
59. German, N.; Kausaite-Minkstimiene, A.; Ramanavicius, A.; Semashko, T.; Mikhailova, R.; Ramanaviciene, A. The use of different glucose oxidases for the development of an amperometric reagentless glucose biosensor based on gold nanoparticles covered by polypyrrole. *Electrochim. Acta* **2015**, *169*, 326–333. [[CrossRef](#)]
60. Apetrei, R.M.; Carac, G.; Bahrim, G.; Ramanaviciene, A.; Ramanavicius, A. Modification of *Aspergillus niger* by Conducting Polymer—Polypyrrole, and the Evaluation of Electrochemical Properties of Modified Cells. *Bioelectrochemistry* **2018**, *121*, 46–55. [[CrossRef](#)]
61. Stirke, A.; Apetrei, R.M.; Kirsnyte, M.; Dedelaite, L.; Bondarenka, V.; Jasulaitiene, V.; Pucetaite, M.; Selskis, A.; Carac, G.; Bahrim, G.; et al. Synthesis of polypyrrole microspheres by *Streptomyces* spp. *Polymer* **2016**, *84*, 99–106. [[CrossRef](#)]
62. Andriukonis, E.; Stirke, A.; Garbaras, A.; Mikoliunaite, L.; Ramanaviciene, A.; Remeikis, V.; Thornton, B.; Ramanavicius, A. Yeast-Assisted Synthesis of Polypyrrole: Quantification and Influence on the Mechanical Properties of the Cell Wall. *Colloids Surf. B Biointerfaces* **2018**, *164*, 224–231. [[CrossRef](#)]

63. Apetrei, R.M.; Carac, G.; Ramanaviciene, A.; Bahrim, G.; Tanase, C.; Ramanavicius, A. Cell-Assisted Synthesis of Conducting Polymer—Polypyrrole—for the Improvement of Electric Charge Transfer through Fungi Cell Wall. *Colloids Surf. B Biointerfaces* **2019**, *175*, 671–679. [[CrossRef](#)]
64. Ramanavicius, A.; Andriukonis, E.; Stirke, A.; Mikoliunaite, L.; Balevicius, Z.; Ramanaviciene, A. Synthesis of Polypyrrole Within the Cell Wall of Yeast by Redox-Cycling of [Fe(CN)₆]³⁻/[Fe(CN)₆]⁴⁻. *Enzym. Microb. Technol.* **2016**, *83*, 40–47. [[CrossRef](#)] [[PubMed](#)]
65. Garbaras, A.; Mikoliunaite, L.; Popov, A.; Ramanaviciene, A.; Remeikis, V.; Ramanavicius, A. Isotope method for the determination of stoichiometry between compounds forming polypyrrole and glucose oxidase composite. *Phys. Chem. Chem. Phys.* **2015**, *17*, 2252–2258. [[CrossRef](#)]
66. Wang, X.; Lu, X.; Wu, L.; Chen, J. Direct electrochemical tyrosinase biosensor based on mesoporous carbon and Co₃O₄ nanorods for the rapid detection of phenolic pollutants. *ChemElectroChem* **2014**, *1*, 808–816. [[CrossRef](#)]
67. Kamysbayev, V.; Filatov, A.S.; Hu, H.; Rui, X.; Lagunas, F.; Wang, D.; Klie, R.F.; Talapin, D.V. Covalent surface modifications and superconductivity of two-dimensional metal carbide MXenes. *Science* **2020**, *369*, 979–983. [[CrossRef](#)]
68. Soomro, R.A.; Jawaid, S.; Zhu, Q.; Abbas, Z.; Xu, B. A mini-review on MXenes as versatile substrate for advanced sensors. *Chin. Chem. Lett.* **2020**, *31*, 922–930. [[CrossRef](#)]
69. Zhu, J.; Ha, W.; Zhao, G.; Huang, D.; Yue, G.; Hu, L.; Sun, N.; Wang, Y.; Lee, L.Y.S.; Xu, C.; et al. Recent advance in MXenes: A promising 2D material for catalysis, sensor and chemical adsorption. *Coord. Chem. Rev.* **2017**, *352*, 306–327. [[CrossRef](#)]
70. Yu, T.; Breslin, C.B. Review—Two-dimensional titanium carbide MXenes and their emerging applications as electrochemical sensors. *J. Electrochem. Soc.* **2020**, *167*, 037514. [[CrossRef](#)]
71. Koyappayil, A.; Chavan, S.G.; Mohammadniaei, M.; Go, A.; Hwang, S.Y.; Lee, M.-H. β-Hydroxybutyrate dehydrogenase decorated MXene nanosheets for the amperometric determination of β-hydroxybutyrate. *Microchim. Acta* **2020**, *187*, 277. [[CrossRef](#)]
72. Zheng, J.; Wang, B.; Ding, A.; Weng, B.; Chen, J. Synthesis of MXene/DNA/Pd/Pt nanocomposite for sensitive detection of dopamine. *J. Electroanal. Chem.* **2018**, *816*, 189–194. [[CrossRef](#)]
73. Sinha, A.; Dhanjai, H.; Zhao, Y.; Huang, X.; Lu, J.; Chen, R.J. MXene: An emerging material for sensing and biosensing. *Trends Anal. Chem.* **2018**, *105*, 424–435. [[CrossRef](#)]
74. Gu, H.; Xing, Y.; Xiong, P.; Tang, H.; Li, C.; Chen, S.; Zeng, R.; Han, K.; Shi, G. Three-Dimensional Porous Ti₃C₂T_x MXene–Graphene Hybrid Films for Glucose Biosensing. *ACS Appl. Nano Mater.* **2019**, *2*, 6537–6545. [[CrossRef](#)]
75. Jiang, Y.; Zhang, X.; Pei, L.; Yue, S.; Ma, L.; Zhou, L.; Huang, Z.; He, Y.; Gao, J. Silver nanoparticles modified two-dimensional transition metal carbides as nanocarriers to fabricate acetylcholinesterase-based electrochemical biosensor. *Chem. Eng. J.* **2018**, *339*, 547–556. [[CrossRef](#)]
76. Song, D.; Jiang, X.; Lu, X.; Luan, S.; Wang, Y.; Li, Y.; Gao, F. Metal_organic frameworks-derived MnO₂/Mn₃O₄ microcuboids with hierarchically ordered nanosheets and Ti₃C₂ MXene/Au NPs composites for electrochemical pesticide detection. *J. Hazard. Mater.* **2019**, *373*, 367–376. [[CrossRef](#)]
77. Lei, Y.; Zhao, W.; Zhang, Y., Jr.; He, H.; Baemner, A.J.; Wolfbeis, O.S.; Wang, Z.L.; Salama, K.N.; Alshareef, H.N. A MXene-based wearable biosensor system for high-performance in vitro perspiration analysis. *Small* **2019**, *15*, 1901190. [[CrossRef](#)]
78. Liu, J.; Jiang, X.; Zhang, R.; Zhang, Y.; Wu, L.; Lu, W.; Li, J.; Li, Y.; Zhang, H. MXene enabled electrochemical microfluidic biosensor: Applications toward multicomponent continuous monitoring in whole blood. *Adv. Funct. Mater.* **2019**, *29*, 1807326. [[CrossRef](#)]
79. Li, Y.; Kang, Z.; Kong, L.; Shi, H.; Zhang, Y.; Cui, M.; Yang, D.P. MXene-Ti₃C₂/CuS nanocomposites: Enhanced peroxidase-like activity and sensitive colorimetric cholesterol detection. *Mater. Sci. Eng. C Mater. Biol. Appl.* **2019**, *104*, 110000. [[CrossRef](#)]
80. Li, H.; Wen, Y.; Zhu, X.; Wang, J.; Zhang, L.; Sun, B. Novel Heterostructure of a MXene@NiFe-LDH Nanohybrid with Superior Peroxidase-Like Activity for Sensitive Colorimetric Detection of Glutathione. *ACS Sustain. Chem. Eng.* **2019**, *8*, 520–526. [[CrossRef](#)]
81. Chen, K.; Qiu, N.; Deng, Q.; Kang, M.-H.; Yang, H.; Baek, J.-U.; Koh, Y.-H.; Du, S.; Huang, Q.; Kim, H.-E. Cytocompatibility of Ti₃AlC₂, Ti₃SiC₂, and Ti₂AlN: In Vitro Tests and First-Principles Calculations. *ACS Biomater. Sci. Eng.* **2017**, *3*, 2293. [[CrossRef](#)]

82. Zong, L.; Wu, H.; Lin, H.; Chen, Y. A polyoxometalate-functionalized two-dimensional titanium carbide composite MXene for effective cancer theranostics. *Nano Res.* **2018**, *11*, 4149–4168. [[CrossRef](#)]
83. Xu, Y.X.; Hu, C.G.; Hu, S.S. A reagentless nitric oxide biosensor based on the direct electrochemistry of hemoglobin adsorbed on the gold colloids modified carbon paste electrode. *Sens. Actuat. B* **2010**, *148*, 253–258. [[CrossRef](#)]
84. Srivastava, P.; Mishra, A.; Mizuseki, H.; Lee, K.R.; Singh, A.K. Mechanistic Insight into the Chemical Exfoliation and Functionalization of Ti_3C_2 MXene. *ACS Appl. Mater. Interfaces* **2016**, *8*, 24256–24264. [[CrossRef](#)]
85. Alhabeab, M.; Maleski, K.; Anasori, B.; Lelyukh, P.; Clark, L.; Sin, S.; Gogotsi, Y. Guidelines for synthesis and processing of two-dimensional titanium carbide (Ti_3C_2T _ MXene). *Chem. Mater.* **2017**, *29*, 7633–7644. [[CrossRef](#)]
86. Sadiq, M.; Pang, L.; Johnson, M.; Sathish, V.; Wang, D. 2D Nanomaterial, Ti_3C_2 MXene-Based Sensor to Guide Lung Cancer Therapy and Management. *Proceedings* **2020**, *60*, 29. [[CrossRef](#)]
87. Ramanavicius, S.; Tereshchenko, A.; Karpicz, R.; Ratautaite, V.; Bubniene, U.; Maneikis, A.; Jagminas, A.; Ramanavicius, A. TiO_{2-x}/TiO_2 -structure based 'self-heated' sensor for the determination of some reducing gases. *Sensors* **2020**, *20*, 74. [[CrossRef](#)]
88. Zhu, Q.; Peng, Y.; Lin, L.; Fan, C.M.; Gao, G.Q.; Wang, R.X.; Xu, A.W. Stable blue TiO_{2-x} nanoparticles for efficient visible light photocatalysts. *J. Mater. Chem.* **2014**, *A2*, 4429–4437. [[CrossRef](#)]
89. Andersson, S.; Magneli, A. Diskrete Titanoxydphasen im Zusammensetzungsbereich $TiO_{1.75}$ - $TiO_{1.90}$. *Naturwissenschaften* **1956**, *43*, 495–496. [[CrossRef](#)]
90. Liborio, L.; Mallia, G.; Harrison, N. Electronic structure of the Ti_4O_7 Magnéli phase. *Phys. Rev. B* **2009**, *79*, 245133. [[CrossRef](#)]
91. Seebauer, E.G.; Kratzer, M.C. Charged point defects in semiconductors. *Mater. Sci. Eng. R Rep.* **2006**, *55*, 57. [[CrossRef](#)]
92. Harada, S.; Tanaka, K.; Inui, H. Thermoelectric properties and crystallographic shear structures in titanium oxides of the Magnéli phases. *J. Appl. Phys.* **2010**, *108*, 083703. [[CrossRef](#)]
93. Smith, J.R.; Walsh, F.C.; Clarke, R.L. Electrodes based on Magnéli phase titanium oxides: The properties and applications of Ebonex[®] materials. *J. Appl. Electrochem.* **1998**, *28*, 1021. [[CrossRef](#)]
94. Walsh, F.C.; Wills, R.G.A. The continuing development of Magnéli phase titanium sub-oxides and Ebonex[®] electrodes. *Electrochim. Acta* **2010**, *55*, 6342. [[CrossRef](#)]
95. Wu, D.; Wang, S.; Zhang, S.; Yuan, J.; Yang, B.; Chen, H. Highly negative Poisson's ratio in a flexible two-dimensional tungsten carbide monolayer. *Phys. Chem. Chem. Phys.* **2018**, *20*, 18924–18930. [[CrossRef](#)]
96. Petruleviciene, M.; Juodkazyte, J.; Parvin, M.; Tereshchenko, A.; Ramanavicius, S.; Karpicz, R.; Samukaite-Bubniene, U.; Ramanavicius, A. Tuning of photo-luminescence properties of WO_3 -based layers by the adjustment of layer formation conditions. *Materials* **2020**, *13*, 2814. [[CrossRef](#)]
97. Ramanavičius, S.; Petrulevičienė, M.; Juodkazytė, J.; Grigučevičienė, A.; Ramanavičius, A. Selectivity of tungsten oxide synthesized by sol-gel method towards some volatile organic compounds and gaseous materials in a broad range of temperatures. *Materials* **2020**, *13*, 523. [[CrossRef](#)]
98. Chen, X.; Sun, X.; Xu, W.; Pan, G.; Zhou, D.; Zhu, J.; Wang, H.; Bai, X.; Dong, B.; Song, H. Ratiometric photoluminescence sensing based on Ti_3C_2 MXene quantum dots as an intracellular pH sensor. *Nanoscale* **2018**, *10*, 1111–1118. [[CrossRef](#)]
99. Ramanaviciene, A.; Ramanavicius, A. Molecularly imprinted polypyrrole-based synthetic receptor for direct detection of bovine leukemia virus glycoproteins. *Biosens. Bioelectron.* **2004**, *20*, 1076–1082. [[CrossRef](#)]
100. Ratautaite, V.; Topkaya, S.N.; Mikoliunaite, L.; Ozsoz, M.; Oztekin, Y.; Ramanaviciene, A.; Ramanavicius, A. Molecularly Imprinted Polypyrrole for DNA Determination. *Electroanalysis* **2013**, *25*, 1169–1177. [[CrossRef](#)]
101. Ramanaviciene, A.; Finkelsteinas, A.; Ramanavicius, A. Basic electrochemistry meets nanotechnology: Electrochemical preparation of artificial receptors based on a nanostructured conducting polymer, polypyrrole. *J. Chem. Educ.* **2006**, *83*, 1212–1214. [[CrossRef](#)]
102. Ratautaite, V.; Janssens, S.D.; Haenen, K.; Nesládek, M.; Ramanaviciene, A.; Baleviciute, I.; Ramanavicius, A. Molecularly Imprinted Polypyrrole Based Impedimetric Sensor for Theophylline Determination. *Electrochim. Acta* **2014**, *130*, 361–367. [[CrossRef](#)]
103. Ma, X.; Tu, X.L.; Gao, F.; Xie, Y.; Huang, X.G.; Fernandez, C.; Qu, F.L.; Liu, G.B.; Lu, L.M.; Yu, Y.F. Hierarchical porous MXene/amino carbon nanotubes-based molecular imprinting sensor for highly sensitive and selective sensing of fisetin. *Sens. Actuators B* **2020**, *309*, 127815. [[CrossRef](#)]

104. Kumar, S.; Lei, Y.; Alshareef, N.H.; Quevedo-Lopez, M.A.; Salama, K.N. Biofunctionalized two-dimensional Ti_3C_2 MXenes for ultrasensitive detection of cancer biomarker. *Biosens. Bioelectron.* **2018**, *121*, 243–249. [[CrossRef](#)]
105. Kulpa, J.; Wojcik, E.; Reinfuss, M.; Kotodziejski, L. Carcinoembryonic antigen, squamous cell carcinoma antigen, CYFRA 21–1, and neuron-specific enolase in squamous cell lung cancer patients. *Clin. Chem.* **2002**, *48*, 1931–1937. [[CrossRef](#)]
106. Wang, S.; Wei, S.; Wang, S.; Zhu, X.; Lei, C.; Huang, Y.; Nie, Z.; Yao, S. Chimeric DNA-functionalized titanium carbide MXenes for simultaneous mapping of dual cancer biomarkers in living cells. *Anal. Chem.* **2019**, *91*, 1651–1658. [[CrossRef](#)]
107. Fang, Y.; Yang, X.; Chen, T.; Xu, G.; Liu, M.; Liu, J.; Xu, Y. Two-dimensional titanium carbide (MXene)-based solid-state electrochemiluminescent sensor for label-free single-nucleotide mismatch discrimination in human urine. *Sens. Actuators* **2018**, *B263*, 400–407. [[CrossRef](#)]
108. Liu, L.; Wei, Y.; Jiao, S.; Zhu, S.; Liu, X. A novel label-free strategy for the ultrasensitive miRNA-182 detection based on $\text{MoS}_2/\text{Ti}_3\text{C}_2$ nanohybrids. *Biosens. Bioelectron.* **2019**, *137*, 45–51. [[CrossRef](#)]
109. Yang, X.; Feng, M.; Xia, J.; Zhang, F.; Wang, Z. An electrochemical biosensor based on AuNPs/ Ti_3C_2 MXene three-dimensional nanocomposite for microRNA-155 detection by exonuclease III-aided cascade target recycling. *J. Electroanal. Chem.* **2020**, *878*, 114669. [[CrossRef](#)]
110. Mohammadniaei, M.; Koyappayil, A.; Sun, Y.; Min, J.; Lee, M.H. Gold nanoparticle/MXene for multiple and sensitive detection of oncomiRs based on synergetic signal amplification. *Biosens. Bioelectron.* **2020**, *159*, 112208. [[CrossRef](#)]
111. Kheyrabadi, L.K.; Koyappayil, A.; Kim, T.; Cheon, Y.-P.; Lee, M.-H. A $\text{MoS}_2@/\text{Ti}_3\text{C}_2\text{T}_x$ MXene hybrid-based electrochemical aptasensor (MEA) for sensitive and rapid detection of Thyroxine. *Bioelectrochemistry* **2021**, *137*, 107674. [[CrossRef](#)]
112. Zhang, H.; Wang, Z.; Zhang, Q.; Wang, F.; Liu, Y. Ti_3C_2 MXenes nanosheets catalyzed highly efficient electrogenerated chemiluminescence biosensor for the detection of exosomes. *Biosens. Bioelectron.* **2019**, *124–125*, 184–190. [[CrossRef](#)]
113. Wang, H.; Li, H.; Huang, Y.; Xiong, M.; Wang, F.; Li, C. A label-free electrochemical biosensor for highly sensitive detection of gliotoxin based on DNA nanostructure/MXene nanocomplexes. *Biosens. Bioelectron.* **2019**, *142*, 111531. [[CrossRef](#)]
114. Chen, L.; Shi, X.; Yu, N.; Zhang, X.; Du, X.; Lin, J. Measurement and Analysis of Thermal Conductivity of $\text{Ti}_3\text{C}_2\text{T}_x$ MXene Films. *Materials* **2018**, *11*, 1701. [[CrossRef](#)]
115. Li, M.H.; Fang, L.; Zhou, H.; Wu, F.; Lu, Y.; Luo, H.J.; Zhang, Y.X.; Hu, B.S. Three-dimensional porous MXene/NiCo-LDH composite for high performance non-enzymatic glucose sensor. *Appl. Surf. Sci.* **2019**, *495*, 143554. [[CrossRef](#)]
116. Dang, Y.; Guan, X.; Zhou, Y.; Hao, C.; Zhang, Y.; Chen, S.; Ma, Y.; Bai, Y.; Gong, Y.; Gao, Y. Biocompatible PB/ Ti_3C_2 hybrid nanocomposites for the non-enzymatic electrochemical detection of H_2O_2 released from living cells. *Sens. Actuators B* **2020**, *319*, 128259. [[CrossRef](#)]
117. Shankar, S.S.; Shereema, R.M.; Rakhi, R.B. Electrochemical determination of adrenaline using MXene/graphite composite paste electrodes. *ACS Appl. Mater. Interfaces* **2018**, *10*, 43343–43351. [[CrossRef](#)]
118. Zhang, Y.; Jiang, X.; Zhang, J.; Zhang, H.; Li, Y. Simultaneous voltammetric determination of acetaminophen and isoniazid using MXene modified screen-printed electrode. *Biosens. Bioelectron.* **2019**, *130*, 315–321. [[CrossRef](#)]
119. Yu, X.; Li, Y.; Cheng, J.; Liu, Z.; Li, Q.; Li, W.; Yang, X.; Xiao, B. Monolayer Ti_2CO_2 : A promising candidate for NH_3 sensor or capturer with high sensitivity and selectivity. *ACS Appl. Mater. Interfaces* **2015**, *7*, 13707–13713. [[CrossRef](#)]
120. Xiao, B.; Li, Y.; Yu, X.; Cheng, J. MXenes: Reusable materials for NH_3 sensor or capturer by controlling the charge injection. *Sens. Actuators B* **2016**, *235*, 103–109. [[CrossRef](#)]
121. Zhao, M.Q.; Ren, C.E.; Ling, Z.; Lukatskaya, M.R.; Zhang, C.; Aken, K.L.V.; Barsoum, M.W.; Gogotsi, Y. Flexible MXene/carbon nanotube composite paper with high volumetric capacitance. *Adv. Mater.* **2015**, *27*, 339–345. [[CrossRef](#)]
122. Mashtalir, O.; Naguib, M.; Mochalin, V.N.; Dall’Agnese, Y.; Heon, M.; Barsoum, M.W.; Gogotsi, Y. Intercalation and delamination of layered carbides and carbonitrides. *Nat. Commun.* **2013**, *4*, 1716. [[CrossRef](#)]
123. Lukatskaya, M.R.; Mashtalir, O.; Ren, C.E.; Dall’Agnese, Y.; Rozier, P.; Taberna, P.L.; Naguib, M.; Simon, P.; Barsoum, M.W.; Gogotsi, Y. Cation intercalation and high volumetric capacitance of two-dimensional titanium carbide. *Science* **2013**, *341*, 1502–1505. [[CrossRef](#)]

124. Choudhary, N.K.; Jin, H.; Kim, B.; Baek, D.S.; Joo, S.H.; Lee, K. MXene: An emerging two-dimensional material for future energy conversion and storage applications. *J. Mater. Chem. A* **2017**, *5*, 24564–24579. [[CrossRef](#)]
125. Ren, C.E.; Zhao, M.-Q.; Makaryan, T.; Halim, J.; Boota, M.; Kota, S.; Anasori, B.; Barsoum, M.W.; Gogotsi, Y. Porous Two-Dimensional Transition Metal Carbide (MXene) Flakes for High-Performance Li-Ion Storage. *ChemElectroChem* **2016**, *3*, 689–693. [[CrossRef](#)]
126. Baniukevic, J.; Boyaci, I.H.; Bozkurt, A.G.; Tamer, U.; Ramanavicius, A.; Ramanaviciene, A. Magnetic gold nanoparticles in SERS-based sandwich immunoassay for antigen detection by well oriented antibodies. *Biosens. Bioelectron.* **2013**, *43*, 281–288. [[CrossRef](#)]
127. Makaraviciute, A.; Ramanaviciene, A. Site-directed antibody immobilization techniques for immunosensors. (A Review). *Biosens. Bioelectron.* **2013**, *50*, 460–471. [[CrossRef](#)]
128. Morkvenaite-Vilkonciene, I.; Ramanaviciene, A.; Kisieliute, A.; Bucinskas, V.; Ramanavicius, A. Scanning electrochemical microscopy in the development of enzymatic sensors and Immunosensors. *Biosens. Bioelectron.* **2019**, *141*, 111411. [[CrossRef](#)]
129. Plikusiene, I.; Balevicius, Z.; Ramanaviciene, A.; Talbot, J.; Mickiene, G.; Balevicius, S.; Stirke, A.; Tereshchenko, A.; Tamosaitis, L.; Zvirblis, G.; et al. Evaluation of affinity sensor response kinetics towards dimeric ligands linked with spacers of different rigidity: Immobilized recombinant granulocyte colony-stimulating factor based synthetic receptor binding with genetically engineered dimeric analyte derivatives. *Biosens. Bioelectron.* **2020**, *156*, 112112.
130. Wang, X.; Garnero, C.; Rochard, G.; Magne, D.; Morisset, S.; Hurand, S.; Chartier, P.; Rousseau, J.; Cabioç'H, T.; Coutanceau, C. A new etching environment (FeF3/HCl) for the synthesis of two-dimensional titanium carbide MXenes: A route towards selective reactivity vs. water. *J. Mater. Chem. A* **2017**, *5*, 22012–22023. [[CrossRef](#)]
131. Wang, H.; Naguib, M.; Page, K.; Wesolowski, D.J.; Gogotsi, Y. Resolving the Structure of $Ti_3C_2T_x$ MXenes through Multilevel Structural Modeling of the Atomic Pair Distribution Function. *Chem. Mater.* **2015**, *28*, 349–359. [[CrossRef](#)]
132. Hope, M.A.; Forse, A.C.; Griffith, K.J.; Lukatskaya, M.R.; Ghidui, M.; Gogotsi, Y.; Grey, C.P. NMR reveals the surface functionalisation of Ti_3C_2 MXene. *Phys. Chem. Chem. Phys.* **2016**, *18*, 5099–5102. [[CrossRef](#)]
133. Zhang, Y.; Zhang, N.; Ge, C. Review First-Principles Studies of Adsorptive Remediation of Water and Air Pollutants Using Two-Dimensional MXene Materials. *Materials* **2018**, *11*, 2281. [[CrossRef](#)]
134. Zheng, J.; Wang, B.; Jin, Y.; Weng, B.; Chen, J. Nanostructured MXene-based biomimetic enzymes for amperometric detection of superoxide anions from HepG2 cells. *Microchim. Acta* **2019**, *186*, 95. [[CrossRef](#)] [[PubMed](#)]
135. Chen, J.L.; Tong, P.; Huang, L.T.; Yu, Z.H.; Tang, D.P. Ti_3C_2 MXene nanosheet-based capacitance immunoassay with tyramine-enzyme repeats to detect prostate-specific antigen on interdigitated micro-comb electrode. *Electrochim. Acta* **2019**, *319*, 375–381. [[CrossRef](#)]

Publisher's Note: MDPI stays neutral with regard to jurisdictional claims in published maps and institutional affiliations.



© 2020 by the authors. Licensee MDPI, Basel, Switzerland. This article is an open access article distributed under the terms and conditions of the Creative Commons Attribution (CC BY) license (<http://creativecommons.org/licenses/by/4.0/>).